Interpolymer Hydrogen-Bonding Complexation Induced Micellization from Polystyrene-*b*-poly(methyl methacrylate) and PS(OH) in Toluene

Shiyong Liu,† Hui Zhu,† Hanyin Zhao,† Ming Jiang,*,† and Chi Wu‡,§

Institute of Macromolecular Science and Laboratory of Molecular Engineering of Polymers, Fudan University, Shanghai 200433, China, Department of Chemistry, The Chinese University of Hong Kong, Shatin, Hong Kong, and The Open Laboratory of Bond-Selective Chemistry, Department of Chemical Physics, University of Science and Technology of China, Hefei, Anhui, China

Received October 1, 1999. In Final Form: January 3, 2000

In this paper, we suggest a new approach to macromolecular assembly by hydrogen-bonding complexation leading to a micelle-like structure from block copolymers in nonselective solvents. The hydrogen bonding between polystyrene-*b*-poly(methyl methacrylate) (PS-*b*-PMMA) and poly{styrene-*co*-[*p*-(2,2,2-trifluoro-1-hydroxy-1-trifluoromethyl)ethyl-α-methylstyrene]} (PS(OH)) in toluene led to a stable core−shell structure with the core and shell, respectively, made of the insoluble PMMA/PS(OH) complexes and the soluble PS blocks as long as the *p*-(2,2,2-trifluoro-1-hydroxy-1-trifluoromethyl)ethyl-α-methylstyrene (HFMS) content of PS(OH) is higher than 8 mol %. Laser light scattering studies found that the molar mass and the core density of the complex micelles increased, but the size decreased as the HFMS content increased. The complexation-induced micelles were very stable, as dilution had almost no effect on them. However, both the size and molar mass of the complex micelles increased as the initial polymer concentration increased, indicating that the complexation was a diffusion-controlled process and the micellization process may not reach thermodynamic equilibrium. In addition, fluorescence and viscometry measurements further supported the concept of formation of hydrogen bonding complex micelles and their dependence on HFMS content in PS(OH).

Introduction

It is well-known that block or graft copolymers can self-assemble in selective solvents to form micelles with a core−shell structure.[1−4] The driving force for micellization is generally attributed to the microphase precipitation of the insoluble blocks and the affinity of the soluble blocks to the solvent. Such micelles, due to their small size (several tens of nanometers) and high stability (low critical micellization concentration),[3−5] may have promising applications in fields such as drug delivery,[6,7] diagnosis,[8] and separation technology.[9] Therefore, micellization of block copolymers in their selective solvents has been extensively studied in the last two decades.

Another effective way of forming block-copolymer micelles, which has been reported only in recent years, is associated with interpolymer complexation. The general idea of the approach is as follows. In a solution blend made of a diblock copolymer A-*b*-B and polymer C, where the solvent is good for A, B, and C, if specific interactions between C and one of the blocks in A-*b*-B leads to an insoluble complex, the complexation can induce the formation of a core−shell micelle-like structure with the complexes as the core and the remaining soluble block as the shell. It is also very well-known that both ionic interactions and hydrogen bonding between complementary polymers result in interpolymer complexes. Recently, Kataoka et al. and Kabanov et al. have successfully investigated a series of a new type of polymer micelles based on interpolymer ionic interactions. Here the block copolymers contain a charged block which forms a complex with an oppositely charged homopolyeletrolyte in water. The reported polymer pairs include poly(ethylene oxide)-*b*-poly(L-lysine)/poly(ethylene oxide)-*b*-poly(α,β-aspartic acid),[10,11] poly(ethylene oxide)-*b*-sodium polymethacrylate/poly(*N*-ethyl-4-vinyl pyridinium),[12] poly(ethylene glycol)-*b*-poly(L-lysine)/oligo-nucleotide,[13] poly(ethylene glycol)-*b*-poly(aspartic acid)/lysozyme,[14] and poly(ethylene oxide)-*b*-polymethacrylate anions/*N*-alkypyridinium cations.[15] This has obviously widened the research area of block-copolymer micellization and shows encouraging prospects in transporting biopolymers[10,13,14] and realizing molecular recognition.[11]

In this paper we report, as a first example, micellization of block copolymers and a random copolymer in a nonselective solvent caused by interpolymer hydrogen-

* To whom correspondence should be addressed.
† Fudan University.
‡ Chinese University of Hong Kong.
§ University of Science and Technology of China.

(1) Halperin, A.; Tirrell, M.; Lodge, T. P. *Adv. Polym. Sci.* **1992**, *100*, 31.
(2) Tuzar, Z.; Kratochivíl, P. In *Surface and Colloid Science*; Matijevic, E., Ed.; Plenum Press: New York, 1993; Vol. 15, p 1.
(3) Webber, S. E. *J. Phys. Chem. B* **1998**, *102*, 2618.
(4) Moffitt, M.; Khougaz, K.; Eisenberg, A. *Acc. Chem. Res.* **1996**, *29*, 95.
(5) Qin, A.; Tian, M.; Ramireddy, C.; Webber, S. E.; Munk, P.; Tuzar, Z. *Macromolecules* **1994**, *27*, 120.
(6) Kataoka, K.; Kwon, G. S.; Yokoyama, Y.; Okano, T.; Sakurai, Y. *J. Contolled Release* **1993**, *24*, 119.
(7) Kwon, G. S.; Kataoka, K. *Adv. Drug Delivery Rev.* **1995**, *16*, 295.
(8) Trubetskoy, V. S.; Frank-Kamenetsky, M. D.; Whiteman, K. R.; Wolf, G. L.; Torchilin, V. P. *Acad. Radiol.* **1996**, *3*, 232.
(9) Nagarajan, R.; Barry, M.; Ruckenstein, E. *Langmuir* **1986**, *2*, 210.
(10) Harada, A.; Kataoka, K. *Macromolecules* **1995**, *28*, 5294.
(11) Harada, A.; Kataoka, K. *Science* **1999**, *283*, 65.
(12) Kabanov, A. V.; Bronich, T. K.; Kabanov, V. A.; Yu, K.; Eisenberg, A. *Macromolecules* **1996**, *29*, 6797.
(13) Kataoka, K.; Togawa, H.; Harada, A.; Yasugi, K.; Matsumoto, T.; Katayose, S. *Macromolecules* **1996**, *29*, 8556.
(14) Harada, A.; Kataoka, K. *Macromolecules* **1998**, *31*, 288.
(15) Bronich, T. K.; Kabanov, A. V.; Kabanov, V. A.; Yu, K.; Eisenberg, A. *Macromolecules* **1997**, *30*, 3519.

10.1021/la9913001 CCC: $19.00
Published on Web 03/09/2000

Scheme 1. Chemical Structure of PS(OH)

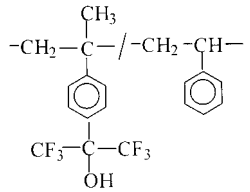

bonding complexation. In fact, the effect of hydrogen bonding on polymer miscibility and interpolymer complexation has been extensively studied with plentiful achievements experimentally and theoretically for almost twenty years.[16−20] In our laboratory, we have concentrated on the blends with controllable hydrogen bonding and found that in such blend solutions, the transition from separated coils to complex aggregates takes place when the density of introduced interaction sites reaches a certain level. For example, in the blend solutions composed of poly(methyl methacrylate) (PMMA) and poly{styrene-*co*-[p-(2,2,2-trifluoro-1-hydroxy-1-trifluoromethyl)ethyl-α-methylstyrene]} (PS(OH)), (Scheme 1), complexation between PS(OH) and PMMA was observed in toluene when the p-(2,2,2-trifluoro-1-hydroxy-1-trifluoromethyl)ethyl-α-methylstyrene (HFMS) content in PS(OH) reached 8 mol %.[18,21] However, the interchain complexes are ill-defined in the microstructure and the precipitation accompanying complexation often made the study of the structure and process difficult. Recently, we prepared soluble complexes with a relatively well-defined structure by grafting polystyrene chains with a functional end group, such as carboxyl or hydroxyl, on poly(4-vinyl pyridine) homopolymers through hydrogen bonding.[22] All these results of our long-term study on miscibility and complexation by hydrogen bonding constructed the basis of our recent study on new approaches to polymer micellization.

Experimental Section

Sample Preparation. Styrene, methyl methacrylate, and *p*-chloro-α-methyl styrene were purified and vacuum distilled in the presence of calcium hydride or/and sodium mirror just before use. The fluorescence energy-donor monomer, vinyl carbazole, from Aldrich was used as received without further purification. The energy-acceptor monomer, 9-anthrylmethyl methacrylate (AMMA), was synthesized as previously described[23] PS-*b*-PMMA copolymers were synthesized by anionic polymerization using *n*-BuLi as the initiator with a sequential addition of styrene and methyl methacrylate.[24] The degree of polymerization of the PS and PMMA blocks were 360 and 240, respectively, determined by both size exclusion chromatography (SEC) and ^{1}H NMR. The polydispersity index (M_w/M_n) was ∼1.2. The hydroxyl-containing monomer *p*-(hexafluoro-2-hydroxyisopropyl)-α-methylstyrene (HFMS) was synthesized from *p*-chloromethylstyrene via Grignard reaction with hexafluoro-acetone. Random copolymers of styrene and HFMS (PS(OH)) were prepared by bulk copolymerization at 60 °C using 2,2-azoisobutyromitrile (AIBN) as the initiator.[21] The products were purified by precipitation in a dichloromethane/petroleum ether mixture. By varying the feed composition, we obtained a series of PS(OH) with the HFMS content in the range of 1.0−50 mol %. Anthracene and carbazole-labeled PS(OH) samples were, respectively, synthesized by copolymerization of HFMS and styrene with a small amount of vinyl carbazole and AMMA. The chromophore contents of the copolymers were around 0.2 wt % determined by UV spectroscopy. Since the content is very low, it would not affect the complexation, viscosity, and light scattering measurements of the copolymers. The HFMS content of a series of carbazole-labeled PS(OH) samples was determined by fluorine analysis. The molecular weights of PS(OH) samples were measured by SEC using a polystyrene calibration. All the results are listed in Table 1. The samples were denoted by PS(OH)-Xa and PS(OH)-Xc where X represents the HFMS content (OH mol %), and c and a, the carbazole and anthracene labels, respectively. The complexation was realized by mixing a proper amount of the PS-*b*-PMMA and PS(OH) toluene solutions. Both the solutions were clarified by a 0.5 μm filter to remove dust before mixing them at ambient temperature.

Table 1. Number-Average Molar Mass (M_n), Polydispersity Index (M_w/M_n), and Chromophore Content of the PS(OH) Samples

sample[a]	OH content	$M_n/10^4$ g/mol	M_w/M_n	chromophore content (wt %)
PS(OH)-1a	1.0	3.2	1.53	0.20
PS(OH)-1c	1.0	3.7	1.63	0.25
PS(OH)-3a	3.2	3.6	1.68	0.18
PS(OH)-3c	3.2	3.8	1.52	0.22
PS(OH)-5a	5.1	2.7	1.64	0.18
PS(OH)-5c	5.1	3.2	1.48	0.22
PS(OH)-8a	8.3	2.8	1.58	0.14
PS(OH)-8c	8.3	3.3	1.40	0.18
PS(OH)-12a	12.4	4.1	1.48	0.16
PS(OH)-12c	12.4	3.4	1.27	0.19
PS(OH)-21a	20.6	1.8	1.59	0.21
PS(OH)-21c	20.6	2.2	1.44	0.23
PS(OH)-34a	33.8	1.5	1.53	0.19
PS(OH)-34c	33.8	1.3	1.52	0.22
PS(OH)-49c	49.2	0.98	1.63	0.22

[a] The numbers denote the mole percentage of the hydroxyl-containing units in PS(OH); a and c respectively denote PS(OH) labeled with 9-anthrylmethyl methacrylate (AMMA) and the vinyl carbazole unit.

Viscosity, Fluorescence, and Laser Light Scattering Measurements. The reduced viscosities of the polymer solution blends in toluene were measured with an Ubbelohde viscometer at 25.0 ± 0.1 °C. The initial concentration of each polymer solution was 4.0×10^{-3} g/mL. The apparent reduced viscosities of the PS-*b*-PMMA/PS(OH)-c blends as a function of the composition were measured 10 min after mixing the PS-*b*-PMMA and PS(OH) solutions.

Fluorescence emission spectra of the polymer solutions were recorded by using a FZ-I fluorescence spectrometer at ca. 25 °C. Each polymer solution was prepared with an oxygen-free solvent. The initial concentrations of PS(OH)-a, and PS(OH)-c and PS-*b*-PMMA were kept at 1.0×10^{-3} g/mL and the solution blends had a volume ratio of [PS(OH)-a + PS(OH)-c]/PS-*b*-PMMA = 2:3, where the ratio of the concentration of vinyl carbazole to that of AMMA was kept at 1/1 (wt/wt). The solutions were purged with N_2 before each measurement. The control experiments were conducted for solutions containing PS(OH)-a and PS(OH)-c with the same concentrations as above by adding pure toluene instead of the PS-*b*-PMMA solution. The wavelength of the excitation light was set at 294 nm and its direction was perpendicular to the detector. The energy transfer efficiency was characterized by the emission intensity ratio of I_c(365 nm) to I_a(416 nm), which were mainly related to the contributions of the energy-donor carbazole and the energy-acceptor anthracene, respectively.

A modified commercial LLS spectrometer (ALV/SP-125) equipped with a multidigital time correlator (ALV-5000E) and a solid-state laser (ADLAS DPY425 II, output power ≅ 50 mW and λ_o = 532 nm) was used. The incident beam was vertically polarized with respect to the scattering plane. All the measure-

(16) Coleman, M.; Graf, J.; Painter, P. *Specific Interactions and the Miscibility of Polymer Blends*; Technomic: Lancaster, PA, 1991.
(17) Pearce, E.; Kwei, T. K.; In *Polymer Solutions, Blends and Interfaces*; Noda, I., Rubingh, D., Eds; Elsevier: Amsterdam, 1992; pp 133−149.
(18) Jiang, M.; Li, M.; Xiang, M.; Zhou, H. *Adv. Polym. Sci.* **1999**, *146*, 121.
(19) Tsuchida, E.; Abe, K. *Adv. Polym.* Sci. **1982**, *45*, 1.
(20) Ting, S. P.; Bulkin, B. J.; Pearce, E. M.; Kwei, T. K. *J. Polym. Sci, Chem. Ed.* **1981**, *19*, 1451.
(21) Qiu, X.; Jiang, M.; *Polymer* **1994**, *35*, 5084.
(22) Liu, S.; Zhang, G.; Jiang, M. *Polymer* **1999**, *40*, 5449.
(23) Stolka, M.; *Macromolecules* **1975**, *8*, 8.
(24) Allen, R. D.; Long, T. E.; Megrath, J. E. *Polym. Bull.* **1986**, *15*, 127.

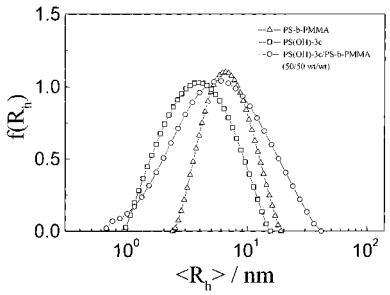

Figure 1. Hydrodynamic radius distributions $f(R_h)$ of PS-*b*-PMMA, PS(OH)-3c and their solution blend (50/50 wt/wt) in toluene, where the total polymer concentration was 1.0×10^{-3} g/mL.

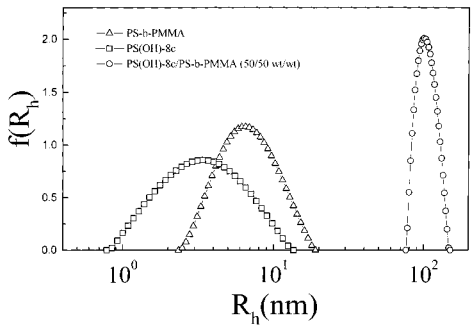

Figure 2. Hydrodynamic radius distributions $f(R_h)$ of PS-*b*-PMMA, PS(OH)-8c and their solution blend (50/50 wt/wt) in toluene, where the total polymer concentration was 1.0×10^{-3} g/mL.

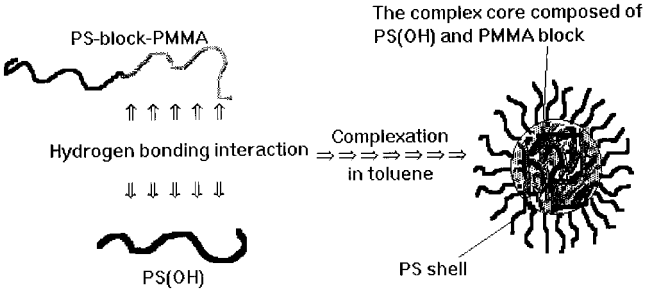

Figure 3. A schematic illustration of the formation of hydrogen-bonded complex micelles from PS-*b*-PMMA and PS(OH).

ments were taken at 25.0 ± 0.01 °C. For PS(OH) with different HFMS content ranging from 0 to 49 mol %, the specific refractive index increment (dn/dC or written as ν) ranges from 0.110 to 0.125 mL/g, while the ν of PMMA is only 0.005 mL/g. Therefore, the light scattered from PMMA can be neglected in comparison with with that from the PS block and PS(OH).

In static LLS, for each solution mixture, the angular dependence of the excess absolute time-averaged scattered intensity, known as the excess Rayleigh ratio $R_{vv}(q)$, was measured. $R_{vv}(q)$ is related to the second virial coefficient A_2, and the z-average root-mean-square radius of gyration $\langle R_g^2 \rangle_z^{1/2}$ (or simply as $\langle R_g \rangle$) as

$$\frac{KC}{R_{vv}(q)} \cong \frac{1}{M_w}\left(1 + \frac{1}{3}\langle R_g^2\rangle_z q^2\right) + 2A_2C \qquad (1)$$

where $K = 4\pi^2 n^2 (\mathrm{d}n/\mathrm{d}c)^2/(N_A\lambda_0^4)$ with N_A, n, and λ_0 being Avogadro's number, the solvent refractive index, and the wavelength of light in a vacuum, respectively, $q = (4\pi n/\lambda_0)\sin(\theta/2)$ with θ being the scattering angle. The polymer concentration (C) is in the units of g/mL. It should be noted that eq 1 is valid only for a homopolymer solution. However, in this study, the values of dn/dc of PS(OH) and PS block are nearly identical, so that we can still use eq 1 for all static LLS if C in eq 1 only refers to the concentration of PS(OH) and PS block of PS-*b*-PMMA.

In dynamic LLS, the intensity−intensity time correlation function $G^{(2)}(q,t)$ was measured in the self-beating mode. The Laplace inversion of $G^{(2)}(q,t)$ led to a line width distribution $G(\Gamma)$. For a diffusive relaxation, Γ is directly related to the translational diffusion coefficient D by $(\Gamma/q^2)_{c\to 0\, q\to 0} = D$. Further, D can be converted to the hydrodynamic radius (R_h) by using the Stokes−Einstein equation, $R_h = k_BT/6\pi\eta D$, where η, k_B, and T are the solvent viscosity, the Boltzmann constant, and absolute temperature, respectively.

Results and Discussion

Laser Light Scattering Study. Differing from our finding in a previous study on conventional complexation that mixing the solutions of homopolymer PMMA and PS(OH) with a HFMS content higher than 8 mol % resulted in a turbid solution or even precipitation,[18,21] mixing block copolymer PS-*b*-PMMA and PS(OH) with different HFMS contents always resulted in transparent solutions, which are stable over months. It means that in the present case, either no strong interchain interactions between the two kinds of polymer chains exist or soluble interchain complexes form. Dynamic light scattering is the most suitable technique to differentiate the two cases since it is sensitive to the existence of large complexes. Figure 1 shows the apparent hydrodynamic radius distributions $f(R_h)$ of PS-*b*-PMMA, PS(OH)-3c and their solution blends (50/50 wt/wt) in toluene. $f(R_h)$ of the blend solution displays a broad peak which resembles a simple additive of the individual PS-*b*-PMMA and PS(OH) chains before mixing, meanwhile, the scattering intensity of the blend solution also shows a simple additivity. This implies that different chains remain nearly independent and there is no evident complexation between the PMMA block and PS(OH). This is attributed to the low HFMS content. However, Figure 2 shows a completely different result as the HFMS content in PS(OH) reaches 8 mol %. The peak position of the PS-*b*-PMMA/PS(OH)-8c solution shifts to ca. 100 nm, and the two peaks associated with the component polymers disappeared. This clearly indicates the occurrence of complexation. A similar phenomenon was also observed when the HFMS content was higher than 8 mol %.

Here, the LLS results have revealed the HFMS content dependence of the complexation between PS(OH) and the PMMA block similar to what we have observed for PS(OH) and poly(alkyl acrylate) homopolymer.[18,21] However, instead of precipitation, the complexation of the block copolymer and PS(OH) resulted in a clear and transparent dispersion over all the composition ranges studied. Since PS blocks have no specific interactions with PS(OH) or the PMMA block, it is reasonable to think that the insoluble PMMA/PS(OH) complexes form the core, which is stabilized by the soluble PS blocks forming a protective shell, as schematically shown in Figure 3.

Table 2 shows that as the HFMS content increases from 8 to 49 mol %, $\langle R_h \rangle$ decreases from ~100 nm to 70 nm while both M_w and N_{agg} increase. Note that the thickness of the PS shell should be almost independent of the HFMS content. Therefore, the decrease of $\langle R_h \rangle$ can only be attributed to the decrease of the core size because the PS(OH) with a high HFMS content can complex more strongly with the PMMA blocks, resulting in a dense core, while for the low HFMS content, a loose structure is present.[21] The values of $\mu_2/\Gamma^2 \le 0.1$ indicate that the complexes are narrowly distributed. In addition, it was observed that Γ/q^2 is independent of the scattering angle indicating that the complexes are spherical.

Figure 4 shows that after the complexation, dilution had nearly no effect on both $\langle R_h \rangle$ and M_w of the PS-*b*-PMMA/PS(OH)-21c (1:1 wt/wt) complex micelles in the

Table 2. Summary of Dynamic and Static LLS Results of the Complexation-Induced Micelles PS-*b*-PMMA/ PS(OH)(50/50wt/wt), Forming in Solutions with Total Polymer Concentration of 1×10^{-3} g/mL

samples	$<R_h>$ nm	M_w 10^7	N_{agg}[a] PS(OH)	N_{agg}[a] PS-*b*-PMMA	$\mu_2/<\Gamma>^{2}$[b]	$<\rho>$[c] g/cm^3
PS(OH)-8c	101	2.8	300	190	0.11	0.011
PS(OH)-21c	84	3.2	500	220	0.08	0.022
PS(OH)-34c	75	3.7	940	250	0.05	0.035
PS(OH)-49c	71	4.9	1530	330	0.07	0.055

[a] N_{agg} is the average number of the chains inside each PS-*b*-PMMA/PS(OH) complexes, which is calculated based on the M_w of complex micelles from LLS and the M_w of PS(OH) and PS block of PS-*b*-PMMA determined from SEC. [b] $\mu_2/<\Gamma>^2$ is the relative width of the line width distribution measured in dynamic LLS. [c] $<\rho>$ is the average density of the complexes defined as $<\rho> = M_w/((4N\pi<R_h>^3)/3)$.

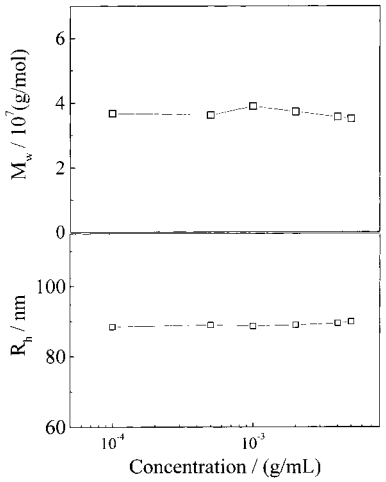

Figure 4. Polymer concentration dependence of $<R_h>$ and apparent weight average molar mass of the complex micelles from PS(OH)-21c/PS-*b*-PMMA (50/50 wt/wt) under dilution.

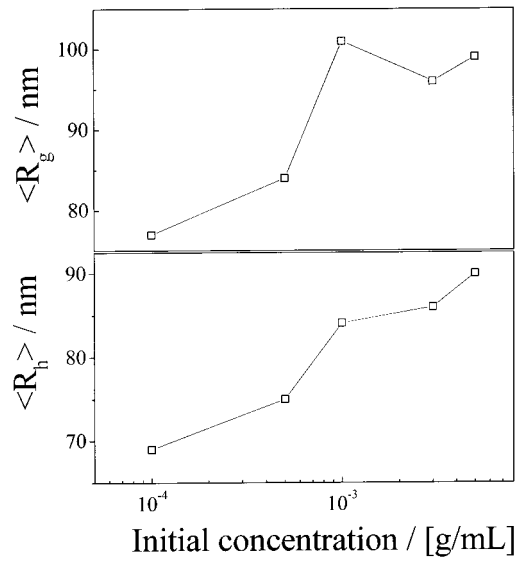

Figure 5. Initial concentration dependence of the average hydrodynamic radius $<R_h>$ of the complex micelles from PS-(OH)-21c and PS-*b*-PMMA (50/50wt/wt).

range of 1×10^{-4} to 5×10^{-3} g/mL. It implies that once the core−shell structures formed, the micelles are kinetically frozen and the chains involved in the micelles do not undergo any spatial rearrangment by dilution. On the other hand, Figures5 and 6 reveal that for the solution blends of PS-*b*-PMMA and PS(OH)-21c prepared with

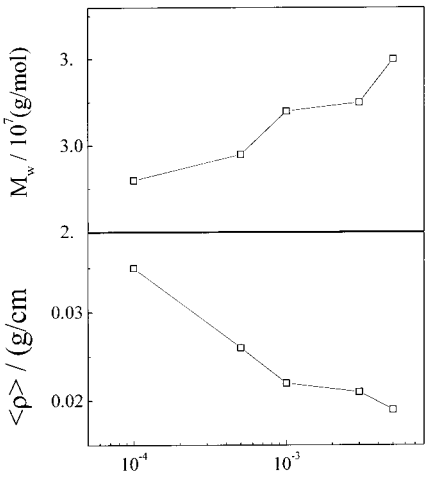

Figure 6. Initial concentration dependence of the weight averaged molar mass M_w and the average chain density $<\rho>$ of the complex micelles from PS(OH)-21c and PS-*b*-PMMA (50/50 wt/wt).

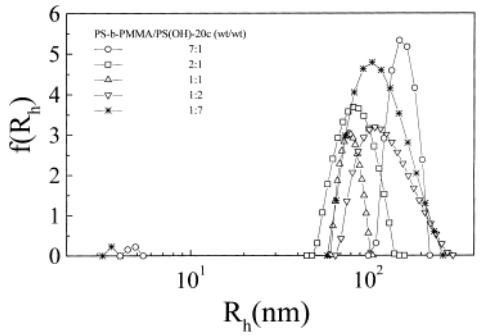

Figure 7. Hydrodynamic radius distribution $f(R_h)$ of the complex micelles of PS(OH)-21c and PS-*b*-PMMA at different mixing ratios. The total polymer concentration is 1×10^{-3} g/mL.

different initial concentration but at a fixed ratio, both the size and molar mass of the complexes decrease but the density increases as the initial concentration decreases. A look at Figures 4−6 clearly shows that the complexation process was kinetically controlled and for the complex micelles, there was no thermodynamic equilibrium between individual interchain complexes and the micelle complexes, just like micelles formed from diblock copolymers in a strong nonsolvent for the core.[1−3]

Figures7 and 8 reveal that at a given total polymer concentration, the PS-*b*-PMMA/PS(OH) ratio dependence of the complexation was complicated. Dynamic LLS results showed that when the ratio of PS-*b*-PMMA to PS(OH) is very asymmetric, i.e., 7:1 and 1:7; in addition to the micelle peak, a small peak located at ∼4 nm was observed, indicating that individual chains exist, while for the ratio ranging between 1:2 and 2:1, nearly all the polymer chains participated in the complexation. Note that when the ratio was around 2:1, R_h was at its lowest, implying a maximum complexation. The variation of the apparent averaged molar mass and $<\rho>$ with the mixing ratio shown in Figure 8 also corroborated this point.

NRET Fluorospectroscopy Studies. Our previous studies on the interchain complexation showed that nonradiative energy transfer (NRET) fluorospectroscopy is an effective method to monitor the formation of the interpolymer complexes and the corresponding changes in the microstructure.[21] It has been known for some time that the energy transfer efficiency between a fluorescent donor and acceptor depends strongly on their proximity to each other over a scale of ∼2−4 nm,[25−28] which is much

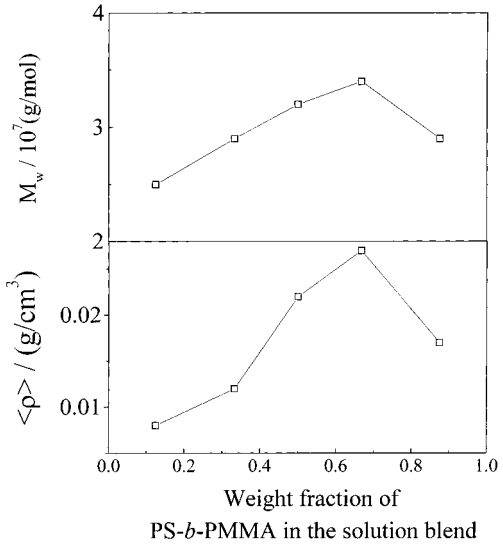

Figure 8. Mixing ratio dependence of the weight averaged molar mass M_w and the average chain density $<\rho>$ of the hydrogen bonded complex micelles from PS(OH)-21c and PS-*b*-PMMA.

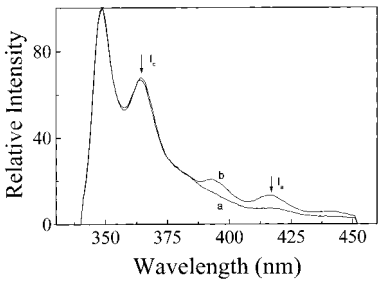

Figure 9. Typical fluorescence emission spectra of (a) PS-*b*-PMMA/[PS(OH)-3a + PS(OH)-3c] solution blend; and (b) PS-*b*-PMMA/[PS(OH)-21a + PS(OH)-21c] solution blend where the weight ratio of [PS(OH)-a + PS(OH)-c]/PS-*b*-PMMA is 2/3 and the weight ratio of vinyl carbazole to that of AMMA was kept at 1/1.

smaller than the diameter of an ordinary polymer chain in solution. Therefore, NRET efficiency may reflect the distance and interpenetration of the two polymer chains, labeled with the energy donor and acceptor. In this study, because both PS(OH)-a and PS(OH)-c chains were complexed with the PMMA block to form the insoluble and collapsed core, an increase of the energy transfer efficiency due to the proximity between the donor and acceptor groups was expected.

Figure 9 shows two typical fluorescence emission spectra for the two solutions in which the respective HFMS contents are 3 mol % and 21 mol %. The evident difference in the emission intensity of the acceptor relative to the donor between the two cases indicates a large difference in the interchain proximity. Figure 10 shows I_c/I_a of the solution blends as a function of HFMS content in PS(OH). In the control experiments where the blend solutions of PS(OH)-a and PS(OH)-c without PS-*b*-PMMA, I_c/I_a remains at a high level and is almost independent of the HFMS content. Note that the ratio of the emission intensities of the donor (I_c, 365 nm) to the acceptor (I_a, 416 nm) is inversely proportional to the energy transfer efficiency. Therefore this result indicates that PS(OH)-a and PS(OH)-c exist as individual chains in dilute solutions. However the solutions containing PS(OH)-a, PS(OH)-c, and PS-*b*-PMMA show completely different behavior. The I_c/I_a value is at a high level only when the HFMS contents are very low, i.e., 1, 3, and 5 mol %. The I_c/I_a ratio dramatically decreases when the HFMS content increases to the range of 8 to 12 mol % and then nearly levels off. This increase of the energy transfer efficiency can be clearly attributed to the accumulation of the PS(OH)-a and PS(OH)-c chains in the micelle cores as both kinds of chains form a complex with the PMMA blocks of PS-*b*-PMMA. Obviously, the fluorescence and LLS results agree with each other and support the schematic illustration shown in Figure 3.

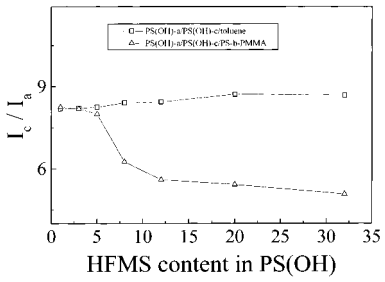

Figure 10. I_c/I_a of [PS(OH)-a + PS(OH)-c]/PS-*b*-PMMA (2/3 wt/wt) blend solutions in toluene as a function of HFMS content in PS(OH), where the weight ratio of vinyl carbazole to that of AMMA was kept at 1/1. PS(OH)-a/PS(OH)-c/toluene blend solutions were used as the control in which the concentration of PS(OH)-a and PS(OH)-c in toluene are the same as that of the solutions containing PS-*b*-PMMA.

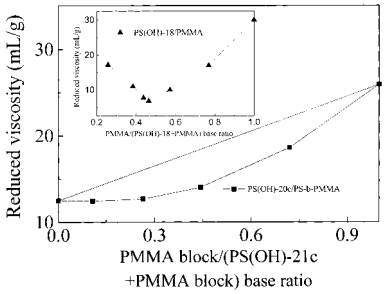

Figure 11. Reduced viscosity of PS(OH)-21c/PS-*b*-PMMA solution in toluene as a function of the PMMA block/(PS(OH)-21c + PMMA block) base ratio. The inset shows the reduced viscosity of PS(OH)-18/PMMA in toluene as a function of PS(OH)-18/PMMA base ratio published in one of our previous papers.[21]

Viscosity Behavior. Viscometry has often been used as an effective method to monitor the interpolymer complexation because the interchain complexation normally leads to a contraction or collapse of the polymer chains and a consequent decrease of solution viscosity.[18−19,21] For example, the complexation between PS(OH) and the PMMA homopolymer and the dependence of complexation on the density of the interaction sites were successfully studied by viscometry.[21] Figure 11 shows that the reduced viscosity of the PS-*b*-PMMA/PS(OH)-21c solution as a function of composition showing a relatively small deviation from the additivity law. For comparison, the inset shows the viscosity variation of the homopolymer PMMA and PS(OH)-18 mixture.[21] It was reported that the mixture of PMMA/PS(OH) with the HFMS content higher than 8% was unstable and turbid. The curve in the inset showed a remarkably negative deviation from the additive law. For the PS-*b*-PMMA/

(25) Jiang, M.; Qiu, X.; Qin, W.; Fei, L. *Macromolecules* **1995**, *28*, 730.
(26) Chen, C. T.; Morawetz, H. *Macromolecules* **1989**, *22*, 159.
(27) Zhu, K. J.; Chen, S. F.; Ho, T.; Pearce, E. M.; Kwei, T. K. *Macromolecules* **1990**, *23*, 150.
(28) Morawetz, H. *J. Polym. Sci. Part A: Polym. Chem.* **1999**, *37*, 1725.

PS(OH)-21c solution blends, at the base mole ratio of PMMA block/PS = 1:1, the reduced viscosity is 14.8 mL/g, 23% smaller than the expected value of 19.1 mL/g by the additivity law while for PMMA/PS(OH)-18 blend at the same base mole ratio, the viscosity decreases to values as low as 7.5 mL/g, 70% lower than the expected value. This difference reflects that although the HFMS content in both cases are similar, the complexation process and structure of the result complexes are different. The block copolymer complex is stable in solution because the insoluble complex core composed of PS(OH) and PMMA blocks is covered and hence stabilized by the soluble PS shells while PMMA/PS(OH) complexes are actually naked particles which readily aggregate and accumulate further to form macroscopic precipitates on standing. In the complexation of PS(OH) and PS-*b*-PMMA, there are three main factors affecting the viscosity as follows: (1) The individual polymer chains combine together forming large particles causing a viscosity increase; (2) Chain collapse accompanying complexation leads to a viscosity decrease; and (3) Extension of the PS chains attached to the micelle cores due to interchain repulsion, just like the polymer brushes grafted on a solid surface and swollen in a good solvent,[1] results in a viscosity increase. The viscosity behavior observed was actually the competing results among the three facts. Obviously, in the case of complexation PS(OH) and PMMA, the absence of the third factor is responsible for the much larger decrease of viscosity in comparison with that of PS-*b*-PMMA and PS(OH).

Conclusions

The complexation between block copolymer polystyrene-*b*-poly(methyl methacrylate) and PS(OH) in toluene results in a stable micelle-like structure with the core and shell made of the insoluble PMMA/PS(OH) complexes and soluble PS blocks, respectively, as long as the HFMS content in PS(OH) is higher than 8 mol %. A combination of static and dynamic light scattering measurements shows that the micelle size decreases while its molar mass and aggregation number increase leading to more dense cores as the HFMS content increases. The micelle-like structures are very stable, as dilution has no effect on their size and mass. However, a decrease of the initial polymer concentration before mixing causes reduction of both the size and molar mass of the complexes, indicating that the complexation is a diffusion-controlled process. The formation of the complex micelles and its dependence on the HFMS content of PS(OH) have been confirmed by the NRET fluorescence measurements. In the viscosity—composition measurements, the complexation between PS(OH) and PS-*b*-PMMA is found to cause a negative deviation from the additivity law. The deviation is much less than that in the PS(OH)/PMMA complexes. All the results show that a micelle-like structure can be obtained in a nonselective solvent for a block copolymer by hydrogen-bonding complexation of one of the blocks and a complementary polymer.

Acknowledgment. This work was supported by National Natural Science Foundation of China (NNSFC, No. 29992590, 59773023), the National Basic Research Project—Macromolecular Condensed State, and the National Distinguished Young Investigation Fund (1996).

LA9913001